Food Chemistry 373 (2022) 131668

Contents lists available at ScienceDirect

Food Chemistry

journal homepage: www.elsevier.com/locate/foodchem

Removal of free fatty acid (FFA) in crude palm oil (CPO) using potassium oxide/dolomite as an adsorbent: Optimization by Taguchi method

I. Nor Shafizah [a,c], R. Irmawati [a,b,c,*], Hishamuddin Omar [d], M. Yahaya [a,e], A. Alia Aina [a]

[a] Department of Chemistry, Faculty of Science, Universiti Putra Malaysia, 43400, UPM Serdang, Selangor, Malaysia
[b] Laboratory of Processing and Product Development, Institute of Plantation Studies, Universiti Putra Malaysia, 43400 UPM Serdang, Selangor, Malaysia
[c] Catalysis Science and Technology Research Centre (PutraCat), Faculty of Science, Universiti Putra Malaysia, 43400, UPM Serdang, Selangor, Malaysia
[d] Department of Biology, Faculty of Science, Universiti Putra Malaysia, 43400, UPM Serdang, Selangor, Malaysia
[e] Desert Research Monitoring and Control Center, Yobe State University, Nigeria

ARTICLE INFO

Keyword:
Deacidification
Free fatty acid
Adsorbent
Crude palm oil
Taguchi

ABSTRACT

In this study, potassium oxide supported on dolomite adsorbent was used as an adsorbent for free fatty acids (FFAs) treatment in crude palm oil (CPO). The characteristics of the adsorbent were determined by TGA, XRD, SEM, BET and TPD-CO_2. Taguchi method was utilized for experimental design and optimum condition determination. There were four parameters and three levels involved in this study: time (30, 60, 90 min), stirring rate (300, 500, 700 rpm), adsorbent dosage (1, 3, 5 wt%) and K_2O concentration (5, 10, 15 wt%). The adsorbent had a larger pore size, higher basic strength, and more basic sites in greater efficiency (63%) in FFAs removal from CPO. The optimum conditions were at 30 min time, 700 rpm stirring rate, 5 wt% adsorbent dosage and 15 wt% K_2O concentration. Taguchi method simplified determination of experimental parameters and minimized the operating costs.

1. Introduction

Palm oil is the premier vegetable oil because of its availability, versatility, nutritional value, and health benefits (Souza Valasques et al., 2020; Sim et al., 2020). Malaysia is one of the top palm oil producers globally with an annual production capacity of approximately 24,000 tonnes (Teh & Lau, 2021; Zhou et al., 2019). Crude palm oil (CPO) is a palm-pressed mesocarp extract comprises oil and water in a fibrous matrix (Teh & Lau, 2021). The vibrant orange colour of CPO comes from its high concentrations of carotenoids, typically ranging from 1200 to 2500 mg/l (Lau, Phuan, Danquah, & Acquah, 2019). It also contains phytonutrients such as tocotrienols, ranging from 1200 to 2000 mg/l (Sulihatimarsyila, Lau, Nabilah, & Azreena, 2020). The FFAs level, the deterioration of bleach ability index (DOBI), iodine value (IV), moisture level, and carotene contents are crucial features to evaluate the quality of CPO (Hew et al., 2020; Sulihatimarsyila et al., 2020). The FFAs content in CPO indicates the deterioration level of oil affects the CPO price in the market (Teh & Lau, 2021). FFAs can alter the taste and give a dreadful flavour and noxious oxygenated compounds (Bao et al., 2019). The crude palm oil mill industries play a vital role in producing high purity and stability palm oil products before transferring them to the palm oil refinery plant. Therefore, to comply with regulation standards, it is essential to keep the FFAs below the specification level, 5% (Bao et al., 2019).

Many researchers have been working on finding a solution for FFAs deacidification in CPO. Chemical refining is a conventional technique for FFAs deacidification which resulting a massive amount of wastewater and soapstock (Shi et al., 2018). On the other hand, physical refining is the alternative way for FFAs deacidification such as distillation, membrane, solvent extraction, enzymatic, and adsorption (Gonçalves, Rodrigues, Marcon, & Meirelles, 2016). The distillation technique usually encounter a problem with evaporated FFAs molecules might condense back to the condenser (Tang et al., 2020). The lipase technique takes a relatively long time and high energy, but it can cause unwanted flavours and aromas (Pootao & Kanjanapongkul, 2016; Sun et al., 2021). Natural solvent consumption should be a concern as well (Werth, Kaupenjohann, Knierbein, & Skiborowski, 2017). Another approach recently described for the removal of FFAs from oils was the use of adsorbents such as TiO_2/chitosan composites fibres (Bao et al., 2019), oil palm boiler ash (OPBA) (Lau et al., 2019), Mg/Silicate (Clowutimon, Kitchaiya, & Assawasaengrat, 2011), etc. Adsorbent treatment has the advantages of reduced oil losses, soap contamination, low cost,

* Corresponding author.
E-mail address: irmawati@upm.edu.my (R. Irmawati).

https://doi.org/10.1016/j.foodchem.2021.131668
Received 29 October 2020; Received in revised form 24 October 2021; Accepted 21 November 2021
Available online 25 November 2021
0308-8146/© 2021 Elsevier Ltd. All rights reserved.

and easy separation by filtration (Resende, Leal, Pereira, Papini, & Magriotis, 2020). The active components of basic metal used on various supports as an adsorbent can improve the reaction rate in sorption activity. There are many reported works on potassium-based adsorbents such as potassium-based aerogel (Guo et al., 2020), potassium-activated geopolymer (Kaewmee, Song, Iwanami, Tsutsumi, & Takahashi, 2020), $K_2W_4O_{13}$ (Huang, Wu, Wei, & Ni, 2019), potassium/zeolite (Gibb, Dynes, & Chang, 2018). The dolomites are noteworthy among the various existing minerals in having several advantageous characteristics such as a high surface area, good structure of porosity, flexibility in tuning physical and chemical properties, mechanical strength, and high availability (Tian et al., 2018). In this study, potassium oxide was the base active component whereas, dolomite was a support material. Some modification on dolomite porous structure with potassium oxide could improve the adsorption efficiencies. Potassium oxide supported on dolomite could have an excellent micro property such as high porosity, high surface area, high pore diameter, and uniform pore structure that could accommodate FFAs molecule for removal.

Statistical tools used in designing the experiments are becoming popular for optimizing the materials. Recent work reported by (Almeida, Santos, Brandão, Korn, & Teixeira, 2019) studied the multivariate optimization of ultrasound-assisted liquid–liquid extraction and determination of metal species such as Cu; Fe, Ni, and Zn in palm oil. They applied a full-factorial design in two levels (2^4) and conducted 20 experiments. They performed a Box-Behnken Response Surface Methodology (RSM) with 15 experimental trials to determine the optimal value for each variable. (Souza Valasques et al., 2020) investigated the optimization by multivariate designs in metal species extraction such as As; Se, and Hg in CPO. They employed a two-level fractional factorial design (2^{5-1}) with 16 experimental trials, Doehlert design with 13 experiments and desirability function in the optimization approach. In the other study, RSM used an analytical tool to examine the 3-Monochloropropane-1,2-diol ester (3-MCPD) removal in CPO (Sim et al., 2020). Four parameters were investigated such as phosphoric acid dosage, degumming temperature, bleaching earth dosage, and deodorization temperature. The response variables were the 3-MCPD ester levels, glycidyl ester levels, colour, and free fatty acid content. Three coded levels (−1, 0, +1) of the process variables were incorporated into the design, resulting in 29 experiment runs. RSM was an experimental design to evaluate the removal of 3-MCPD in CPO in the presence of bleaching earth as an adsorbent (Hew et al., 2020). The optimum conditions were determined by using statistical analysis. There were two parameters involved (type of adsorbent and adsorbent dosage) which require 18 trial runs for the experiment. ANOVA was used to the responses to create statistical and diagnostic models. In addition, the Taguchi method also has been widely used for the experiment design and optimization phase of the independent variables and affecting dependent variables. (Singh & Verma, 2019) integrate the Taguchi method and RSM in their study. Taguchi method was employed to design the experimental. Whereas RSM was applied to determine the optimum parameters in biodiesel production. L27 orthogonal array design constructed consists of three levels and six factors for the experimental runs.

Taguchi is a well-known approach for optimization as it rapidly establishes the desired result with lesser interaction of parameters (Singh & Verma, 2019). The regression model was statistically using analysis of variance (ANOVA) to evaluate the relevance of studied parameters (Zhang, Wang, & Yang, 2021). ANOVA would allow the computation of signal to noise ratio (SNR) depending on the results obtained from experiments to the standard deviation. SNR determine the optimum level of each parameter along with its respective set of optimum conditions to maximize the efficiency of the process (Dhawane et al., 2018). There are three types of SNR analyses that are generally applicable: the higher-the-better (HTB), nominal-the-better (NTB) and lower-the-better (LTB). For this case, the HTB formula will utilize attributes to maximum FFAs reduction percentage in CPO deacidification. The signals are indicators of the effect on average responses. The noises are measures of the influence on the deviations from the sensitivity of the dependent variables to noise factors (Zhang et al., 2021). In this work, even though the process of the adsorption test is simple. There are four parameters (time, stirring rate, adsorbent dosage, and K_2O concentration) involved in this study which might require a lengthy trial. The Taguchi method could reduce the number of experiments and achieve the optimum results in a short duration for this study. Hence, this paper presented the optimization study on adsorbent efficiency on FFAs removal using potassium oxide/dolomite as an adsorbent.

2. Material and methods

2.1 Materials and reagents

Crude palm oil (CPO) was obtained from Sime Darby Research Sdn. Bhd, Selangor, Malaysia. The dolomite was supplied by Northern Dolomite Sdn. Bhd., Perlis, Malaysia. The dolomite was grinded and sieved (350 μm mesh size) before use. Potassium carbonate (K_2CO_3), 99.5%, (R&M chemicals, Selangor, Malaysia), Isopropanol ($CH_3CH_2CH_2OH$), 99.70% (Sigma-Aldrich, Selangor, Malaysia) and ethanol (CH_3CH_2OH), 99.7% (Sigma-Aldrich, Selangor Malaysia) were supplied by Laboratory and Scientific Enterprise, Selangor, Malaysia. Potassium hydroxide (KOH), 99.0% (Systerm, Selangor, Malaysia) and Phenolphthalein (Systerm, Selangor, Malaysia) were supplied by LGC Scientific Sdn. Bhd, Selangor, Malaysia. All chemicals and solvents were used without any purification involved.

2.1. Adsorbent synthesis

5 wt% of potassium carbonate diluted in an appropriate volume of deionized water. The solution was poured into 50 g of calcined dolomite powder. The mixture was stirred at 350 rpm for 30 min until it was homogeneous. The mixture was placed into the oven and heated at a temperature of 110 °C overnight. The dried sample was grinded and sieved using mesh (size: 350 μm) to turn it into a fine powder. The sample was then calcined in a furnace at a temperature of 850 °C for 4 h. The sample was denoted as 5 wt% K_2O/dolomite. The procedure steps repeated for another K_2O concentration on dolomite such as 10 wt% and 15 wt%. These samples were denoted as 10 wt% K_2O/dolomite and 15 wt% K_2O/dolomite, respectively.

2.2. Characterization of adsorbent

The thermal stability of the adsorbent was assessed by using a Mettler Toledo TG-SDTA apparatus (Pt crucibles, Pt/Pt–Rh thermocouple). The analysis was purged under nitrogen (N_2) gas at a flow rate of 30 ml/min, heating rate of 10 °C/min, and temperature ranging from room temperature to 1000 °C. The XRD analysis was performed using a Shimadzu diffractometer model XRD-6000 (Shimadzu Chiyoda-ku Tokyo). XRD patterns were generated using CuK_α radiation ($\lambda = 1.541°$) at 30 kV, current of 30 mA, and at scanning speed of 2°/min. The rate scanning was 20° to 80° in term of 2θ. The diffractograms produced were matched with the published International Centre for Diffraction Data. The In-lens SE detector (TLD-SE) will capture various signals. The pore size and pore volume distribution of the adsorbent were determined by the amount of gas desorbed from the adsorbent surface at the boiling point of N_2 (−196 °C). The Brunauer-Emmett-Teller (BET) analysis was conducted by using MicroActive for TriSstar II Plus Version 2.03 for surface area and porosity determination. The standard measuring points used in the device are 0.1, 0.2, and 0.3P/P_o. The adsorbent was dried at 70 °C with 10 °C/min ramp temperature and 760 torr pressures. The TPD-CO_2 analysis performed using a Thermo Finnigan TPD/R/O 1100 instrument equipped with a thermal conductivity detector (TCD). 0.05 g of the sample was inserted into the sample vessel and purged with N_2 for 30 min at 250 °C. The adsorbent was then exposed to carbon dioxide (CO_2) gas for 1 h at ambient temperature to allow adsorption of CO_2 onto the sample's surface. Excessed CO_2 was subsequently flushed by N_2

gas. The desorption of CO_2 from the basic sites of adsorbent was detected by TCD under Helium (He) gas flow (30 ml/min) from 50 °C to 1000 °C and temperature was held for 30 min. SEM analysis was carried out using an FEI Nova NanoSEM230 model operated at 1.0 kV to 15.0 kV. The adsorbent's morphology was captured at magnifications of 25,000x.

2.3. Adsorbent test

50 g of raw CPO was poured into an Erlenmeyer flask and preheated in a silicon bath at a temperature of 80 °C for 30 min under a continuous stirring rate of 500 rpm. The adsorbent added into the preheated CPO and the adsorption begun. The mixture stirred at 500 rpm for 30 min. When the adsorption test finished, the adsorbent was separated from treated CPO by centrifugation at 1000 rpm for 10 min. The experiments repeated according to the orthogonal array by Taguchi method shown in Table 1. The acid value titration performed to determine the acid value of the treated CPO. The acid value measured by using equation (Eq. (1)). Whereas the FFA reduction percentage was determined using this equation (Eq. (2)) as below:

$$Acid\ value = \frac{Normality\ of\ KOH \times (volume\ treated\ CPO - volume\ blank) \times molar\ mass\ KOH}{Weight\ of\ CPO} \quad (1)$$

$$FFA\ reduction\ (\%) = \frac{Acid\ value\ raw\ CPO - Acid\ value\ treated\ CPO}{Acid\ value\ raw\ CPO} \quad (2)$$

2.4. Design of experiment (DOE) using Taguchi method

There are four parameters investigated at selected three levels which are A: time (30, 60, 90 min), B: stirring rate (300, 500, 700 rpm), C: adsorbent dosage (1, 3, 5 wt%), D: K_2O concentration (5, 10, 15 wt%). Based on these parameters, the L9 (3^4) was selected. The adsorbent trials performed according to the orthogonal array (Table S1 supplemental files). The data obtained in percentage (%) converted into SNR and inserted into the database system (Stat-Ease Design Expert 6.0.6). For each parameter, the contribution factor gives the idea of its effect on the process and can be assessed by Eq. (3):

$$\%contribution\ of\ factor = \frac{SS_f}{SS_T} \times 100 \quad (3)$$

where, for the fth variable, SS_f = the sum of squares and SS_T = the sum of squares of all variables.

Table 1
BET surface and porosity and TPD profiles of the K_2O, calcined dolomite, synthesized adsorbents.

Type	BET surface area (m^2/g)	Pore volume (cm^3/g)	Pore size (nm)	Max Temp (K)	Total amount of CO_2 desorbed (μmol/g)
K_2O	0.4	0.0010	1.7	–	–
Calcined dolomite	19.1	0.0340	5.7	601, 621	501.4
5 wt% K_2O/ dolomite	6.9	0.0240	6.1	601, 693	892.2
10 wt% K_2O/ dolomite	5.2	0.0190	6.0	604, 648, 720	1692.5
15 wt% K_2O/ dolomite	4.2	0.0150	6.1	607, 683, 755	3165.2

The regression model was determined using ANOVA and studied the correlation of the expected response. The optimum condition was forecasted by choosing the maximum target for significant factors and the minimum target for insignificant factors. The forecasted optimized conditions were validated with experimental runs in triplicates for checking variations between actual and expected responses.

3. Results

3.1. Physicochemical properties of synthesized adsorbents

The thermal behaviour (Fig. 1S in supplemental files) of K_2O/dolomite adsorbents of all concentrations showed a similar pattern. Three stages of weight loss between 100 °C and 1000 °C. The commencement of the decomposition for K_2O/dolomite adsorbents occurred only above 400 °C. Thereafter, the TG curve for calcined dolomites and K_2O/dolomite adsorbents seemed to level off between the temperatures between 600 °C and 800 °C. The weight loss of the dolomite and all adsorbents against temperature remained almost constant indicating excellent thermal stability where they can potentially utilize for industrial CPO milling or refining which normally operates below 100 °C. The weight loss of adsorbent at 800 °C decreases as the K_2O loading on the dolomite increases. The addition of K_2O helps in stabilizing the surface of dolomites and hence improve the thermal stability of the synthesized adsorbents.

The diffractograms of calcined dolomite and K_2O/dolomite adsorbents illustrated in Fig. 1. Two intense peaks observed for dolomite diffraction peak at 2θ = 43.5° and 62° (JCPDS File No.:00-075-1525) attributes to high crystallinity of quicklime (CaO) and periclase (MgO). Both compounds have a cubic crystal structure (Mohammed, Shafizah, Salmiaton, & Azlina, 2020). K_2O peak was observed at 2θ = 33.1° (JCPDS File No.:00-025-0626). The diffractogram of 5 wt% K_2O/dolomite, however, changes drastically compared to the calcined dolomite. Intense peaks that belonged to CaO and MgO exhibited major shifting for K_2O/dolomite adsorbents. Moreover, the intensity of CaO and MgO of the loaded adsorbents reduced when K_2O introduced onto dolomite. K_2O peak shifted slightly at 2θ = 35.0° and 36.1° (JCPDS File

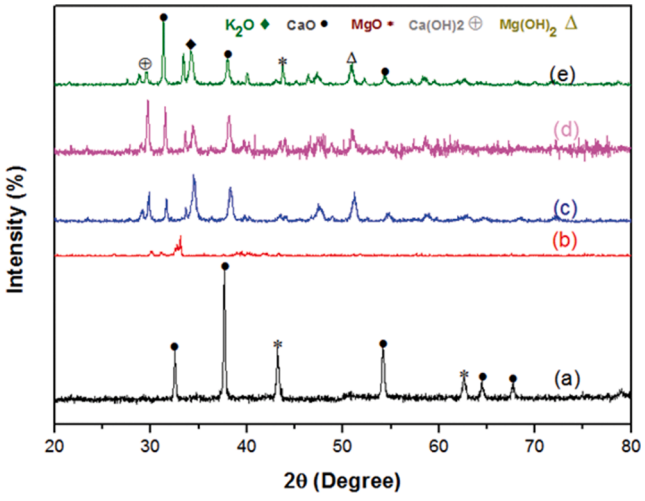

Fig. 1. XRD profile dolomite, (a) calcined dolomite, (b) K_2O (c) 5 wt% K_2O/dolomite, (d) 10 wt% K_2O/dolomite, (e) 15 wt% K_2O/dolomite adsorbent.

No.:00-025-0626) attributes to a new arrangement in atomic structure.

The surface area, pore-volume, and pore size K_2O, calcined dolomite, and all synthesized adsorbents tabulated the Table 1. Adding the K_2O on dolomite drastically reduced the adsorbent's surface area and pore volume. Further increment in K_2O loading has affected the adsorbent's surface area and pore more. According to (Yahaya et al., 2020), it is expected that after the calcination of dolomite, the compounds ($CaMg(CO_3)_2$) transform into CaO and MgO and create pores which will enhance the surface area. However, the insertion of K_2O into the dolomite structure has occupied and blocked the channels hence reduces the pore volume. In addition, the covering of the outer surface of the adsorbent results in a drastic reduction in the surface area. The reduction of the surface area values of all adsorbents was anticipated and synchronized with pore volume. The K_2O addition on dolomites has improved the adsorbent's pore size. However, it is unchanged at different K_2O concentration levels. All adsorbents can accommodate the oil molecules (2 nm in size) and allow for adsorption activities to occur. The insertion of K_2O might have filled the small pores. However, the insertion might have improved the remaining larger pores on the surface.

The total number of base sites and their relative strength which was measured through a total amount of CO_2 desorbed were tabulated in Table 1. All synthesized adsorbents (Fig. 2S in supplemental files) have high strength of basicity when K_2O incorporated into dolomite structure. From the result displayed, calcined dolomite has a strong strength of basicity and density of basic sites of 501.4 μmol/g. However, the addition of K_2O has increased the basic strength and create very strong base sites on the surface of dolomite. The density of basic sites attributes to the availability of adsorption sites on the adsorbent surface which shows an increment towards the addition of K_2O concentration which are 892.2, 1692.5, and 3165.2 μmol/g for 5, 10, and 15 wt% K_2O/dolomite, respectively. The high K_2O concentration remarkably increases the basic sites due to the interaction effect of K_2O, MgO, and CaO (Yahaya et al., 2020).

The results displayed (Fig. 3S in supplemental files) a similar morphology of the microstructure surface of K_2O/dolomite. The formation of coarse particle is randomly distributed and showing the lack of proper molecules ordering and rearrangement. These segregated particles contribute to a low BET surface area for all adsorbents. However, at some parts of the structures are exhibiting the open subsets while at other parts acted as a closed surface without any boundaries between it. As depicted in the SEM images, adsorbents are not in a very porous structure.

3.2. Adsorbent test of FFAs reduction in CPO

The adsorbent test for FFAs removal in CPO using K_2O/dolomite adsorbents performed according to the L9 orthogonal array by Taguchi Method shown in Table 2. The experimental trials replicated three times (FFA1, FFA2, and FFA3). The response in this study determined by signal to noise ratio (SNR). The highest FFAs reduction achieved at 63%

Table 2
L9 DoE for FFAs removal in CPO using synthesized K_2O/dolomite absorbents.

No	(A)	(B)	(C)	(D)	FFA1	FFA2	FFA3	SD	SNR
1	30	500	3	10	45.2	45.3	45.6	0.21	33.1
2	60	700	1	10	39.1	39.6	39.4	0.26	31.7
3	60	500	5	5	32.2	32.6	32.6	0.23	30.2
4	60	300	3	15	51.7	51.3	51.5	0.20	34.2
5	30	300	1	5	27.4	27.6	27.1	0.25	28.8
6	90	300	5	10	52.4	52.6	52.7	0.15	34.2
7	30	700	5	15	63.4	63.4	63.6	0.12	36.0
8	90	700	3	5	32.1	32.5	32.6	0.26	30.0
9	90	500	1	15	37.4	37.8	37.5	0.21	31.5

A: time; B: stirring rate; C: adsorbent dosage; D: K_2O concentration.
$FFAs_n$: Free fatty acid; SD: Standard deviation; SNR: Signal to Noise ratio.

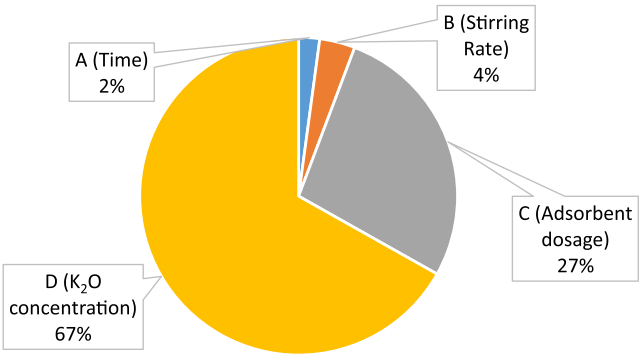

Fig. 2. Percentage contribution of all factors.

at optimum conditions; time 30 min, stirring rate of 700 rpm, the adsorbent dosage of 5 wt% and K_2O concentration of 15 wt%. On the other hand, the lowest FFAs reduction achieved at 27% at conditions; time 30 min, stirring rate of 300 rpm, adsorbent dosage of 1 wt% and K_2O concentrations of 5 wt%.

Fig. 2 illustrates the percentage of contribution for all factors. Any selection of more than 5% will be known as the significant factor toward the adsorption activity. Meanwhile, any selection less than 5% levels will have less influence on the adsorption activity. The K_2O concentration and adsorbent dosage are the major contributions in adsorption activity with 67% and 27%, respectively. Meanwhile, the least significant factors are time and the stirring rate with 2% and 4%, respectively. Both values identified below the acceptance level (<5%).

The analysis of variance (Table 21 in supplemental files) for all parameters and levels of the experiment shows there is only a 0.95% probability that this high "Model F-value" will occur because of noise. 'Prob > F' values lower than 0.05 mean that the terms of the model are important. In this case, the significant factors are adsorbent dosage and K_2O adsorbent concentration. The 'Pre R-Squared' of 0.7097 is in reasonable agreement with the 'Adj R-Squared' of 0.8853. Adjusted R-squared values explain the degree to which the input of independent variables explain the variation of the dependent variable, and they indicated that the predictions of the dependent variables based on the ANOVA (Zhang et al., 2021). "Adeq Precision" shows an adequate signal which is an 11.81 ratio which is above the desirable level (greater than 4). This model possibly can be used to navigate the design space.

The distribution of nine sets of conditions displayed (Fig. 4S in supplemental files) in predicted and actual SNR. A straight line that is directly proportional is at the centre of the graph, which corresponds to the best line fit. In that case, all points should be on the line passing through the origin and tilted to 45° to indicate the perfect correlation data. However, about five of nine points lie on the line, while the other four points were distributed slightly closer surrounding the straight line.

Fig. 3 reveals the effect of significant factors on the FFAs reduction percentage. The percentage contribution of the adsorbent dosage during the adsorption test plays an important role in increasing and decreasing the FFAs reduction level. As depicted in Fig. 3a, that an increase of the adsorbent dosage from 1 wt% to 3 wt% resulted in a higher FFAs reduction from 37% to 51%, while a further increase till 5 wt% resulted in an increase of FFAs reduction to 63%. It may be due to more available adsorption capacity for FFAs adsorption. FFAs molecules will have extra sufficient contact on the surface of the adsorbent. Hence, the rancidity of the CPO would reduce by an increase in the FFAs reduction percentage. Owing to that, the optimum condition for the adsorbent dosage is 5 wt%. Another important aspect is the K_2O concentration shown in Fig. 3b. Increase the K_2O concentration from 5 wt% to 10 wt% resulted in an increase FFAs reduction from 32% to 52%, while a further increase to 15 wt% resulted in a higher FFAs reduction to 63%. This outcome due to the availability of adsorption sites which was observed in TPD of the synthesized adsorption. The increment in adsorption sites as the K_2O

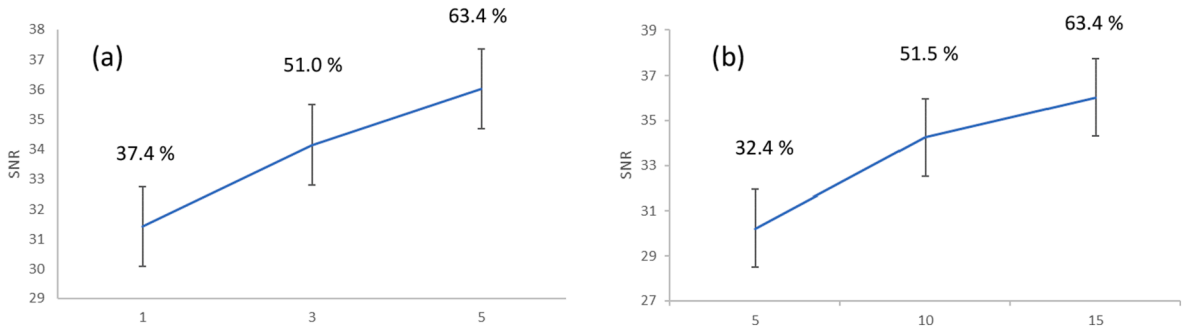

Fig. 3. Effect of significant parameter (a) Adsorbent dosage (b) K_2O concentration.

concentration increase was in line with the FFAs adsorption activities. Moreover, the availability of pores occupied with K_2O as the K_2O loaded onto dolomite might explain the higher FFAs reduction. The optimum K_2O concentration is 15 wt%.

The suggested experimental condition by Taguchi was validated by experimenting twice (Table 3S supplemental files). The operating condition finalized by selecting the optimum level for significant factors and the least level for insignificant factors. Since time and the stirring rate has the least impact on the adsorption activity, the validation test conducted at lower conditions at 30 min time and stirred at 300 rpm. Taguchi method reduces the cost, operation time, and energy consumption. However, adsorption activity conducted at the selected optimum level of adsorbent dosage (5 wt%) and K_2O concentration (15 wt %) to achieve higher FFAs reduction. From the table, trial 2 shows that SNR obtained is more precise than trial 1. The percentage deviation error was only 0.3%.

3.3. Conclusion

In conclusion, the K_2O/dolomite is an alternative adsorbent for FFAs treatment in CPO. The adsorbents have high thermal stability up to 800 °C. The addition of K_2O onto the dolomite improved the porosity of the synthesized K_2O/dolomite adsorbent. Increasing the K_2O concentration on dolomites resulted in decreasing the surface area and pore volume. However, it resulted in increasing the pore size and the density of adsorption basic sites. 15 wt% K_2O/dolomite adsorbent has the highest pore size (6.1 nm), basicity strength and degree of basicity (3165.2 μmol/g). Adsorbent dosage (27% contribution) and K_2O concentration (67% contribution) are the significant factors in the FFAs reduction, while time and stirring rate were the least influential factors in the FFAs adsorption test. The optimum conditions for FFAs reduction in CPO determined by the Taguchi method. The highest FFAs reduction (63%) was achieved at optimum conditions: time of 30 min, stirring rate of 300 rpm, 5 wt% of adsorbent dosage and 15 wt% of K_2O concentrations.

CRediT authorship contribution statement

I. Nor Shafizah: Conceptualization, Data curation, Formal analysis, Investigation, Methodology, Project administration, Software, Visualization, Writing – original draft. **R. Irmawati:** Conceptualization, Funding acquisition, Investigation, Methodology, Project administration, Resources, Supervision, Validation, Visualization, Writing – review & editing. **Hishamuddin Omar:** Funding acquisition, Investigation, Methodology, Project administration, Resources, Validation. **M. Yahaya:** Data curation, Formal analysis, Software. **A. Alia Aina:** Data curation, Formal analysis, Writing – original draft.

Declaration of Competing Interest

The authors declare that they have no known competing financial interests or personal relationships that could have appeared to influence the work reported in this paper.

Acknowledgement

This research was funded by Putra High-Impact Grant (Vote No. GPB :9658900) from Universiti Putra Malaysia.

Appendix A. Supplementary data

Supplementary data to this article can be found online at https://doi.org/10.1016/j.foodchem.2021.131668.

References

Almeida, J. S., Santos, G. L., Brandão, G. C., Korn, M. G. A., & Teixeira, L. S. G. (2019). Multivariate optimization of ultrasound-assisted extraction using Doehlert matrix for simultaneous determination of Fe and Ni in vegetable oils by high-resolution continuum source graphite furnace atomic absorption spectrometry. *Food Chemistry, 273*, 130–135. https://doi.org/10.1016/j.foodchem.2018.01.112

Bao, Y., Zhou, Q., Zhang, M., Zhang, H., Luan, Q., Zhou, W., & Tang, H. (2019). Wet-spun nanoTiO2/chitosan nanocomposite fibers as efficient and retrievable absorbent for the removal of free fatty acids from edible oil. *Carbohydrate Polymers, 210*(January), 119–126.

Clowutimon, W., Kitchaiya, P., & Assawasaengrat, P. (2011). Adsorption of free fatty acid from crude palm oil on magnesium silicate derived from rice husk. *Engineering Journal, 15*(3), 15–26. https://doi.org/10.4186/ej.2011.15.3.15

Dhawane, Sumit H., Karmakar, Bisheswar, Ghosh, Shubham, & Halder, Gopinath (2018). Parametric optimisation of biodiesel synthesis from waste cooking oil via Taguchi approach. *Journal of Environmental Chemical Engineering, 6*, 3971–3980.

Gibb, N. P., Dynes, J. J., & Chang, W. (2018). Chemosphere A recyclable adsorbent for salinized groundwater : Dual-adsorbent desalination and potassium-exchanged zeolite production. *Chemosphere, 209*.

Gonçalves, C. B., Rodrigues, C. E. C., Marcon, E. C., & Meirelles, A. J. A. (2016). Deacidification of palm oil by solvent extraction. *Separation and Purification Technology, 160*, 106–111. https://doi.org/10.1016/j.seppur.2016.01.016

Guo, B., Wang, Y., Guo, J., Qiao, X., Zhang, M., & Jin, Y. (2020). Experiment and kinetic model study on modified potassium-based CO2 adsorbent. *Chemical Engineering Journal, 399*(March).

Hew, K. S., Asis, A. J., Tan, T. B., Yusoff, M. M., Lai, O. M., Nehdi, I. A., & Tan, C. P. (2020). Revising degumming and bleaching processes of palm oil refining for the mitigation of 3-monochloropropane-1,2-diol esters (3-MCPDE) and glycidyl esters (GE) contents in refined palm oil. *Food Chemistry, 307*(May 2019). https://doi.org/10.1016/j.foodchem.2019.125545

Huang, Q., Wu, W., Wei, W., & Ni, B. (2019). Polyethylenimine modified potassium tungsten oxide adsorbent for highly efficient Ag+ removal and valuable Ag0 recovery. *Science of the Total Environment, 692*, 1048–1056.

Kaewmee, P., Song, M., Iwanami, M., Tsutsumi, H., & Takahashi, F. (2020). Porous and reusable potassium-activated geopolymer adsorbent with high compressive strength fabricated from coal fly ash wastes. *Journal of Cleaner Production, 272*.

Lau, S. Y., Phuan, S. L., Danquah, M. K., & Acquah, C. (2019). Sustainable palm oil refining using pelletized and surface-modified oil palm boiler ash (OPBA) biosorbent. *Journal of Cleaner Production, 230*, 527–535. https://doi.org/10.1016/j.jclepro.2019.04.390

Mohammed, M. A. A., Shafizah, I. N., Salmiaton, A., & Azlina, W. A. K. G. W. (2020). The evaluation on three types of Malaysian Dolomites as a primary catalyst in gasification reaction of EFB and tar cracking efficiency. *Frontiers in Energy Research, 8*(March), 1–11. https://doi.org/10.3389/fenrg.2020.00038

Pootao, S., & Kanjanapongkul, K. (2016). Effects of ohmic pretreatment on crude palm oil yield and key qualities. *Journal of Food Engineering, 190*, 94–100. https://doi.org/10.1016/j.jfoodeng.2016.06.021

Resende, R. F., Leal, P. V. B., Pereira, D. H., Papini, R. M., & Magriotis, Z. M. (2020). Removal of fatty acid by natural and modified bentonites: Elucidation of adsorption mechanism. *Colloids and Surfaces A: Physicochemical and Engineering Aspects, 605* (July). https://doi.org/10.1016/j.colsurfa.2020.125340

Shi, L., Zheng, L., Zhao, C., Huang, J., Jin, Q., & Wang, X. (2018). Effects of deacidification methods on high free fatty acid containing oils obtained from sea buckthron (Hippophaë rhamnoides L.) berry. *Industrial Crops and Products, 124* (July), 797–805.

Sim, B. I., Khor, Y. P., Lai, O. M., Yeoh, C. B., Wang, Y., Liu, Y., … Tan, C. P. (2020). Mitigation of 3-MCPD esters and glycidyl esters during the physical refining process of palm oil by micro and macro laboratory scale refining. *Food Chemistry, 328* (March). https://doi.org/10.1016/j.foodchem.2020.127147

Singh, T. S., & Verma, T. N. (2019). Taguchi design approach for extraction of methyl ester from waste cooking oil using synthesized CaO as heterogeneous catalyst: Response surface methodology optimization. *Energy Conversion and Management, 182* (January), 383–397. https://doi.org/10.1016/j.enconman.2018.12.077

Souza Valasques, G., Maria Pinto dos Santos, A., Levi França da Silva, D., Mozart Ferreira da Mata Cerqueira, U., Luis Costa Ferreira, A., Nei Lopes dos Santos, W., & Almeida Bezerra, M. (2020). Extraction induced by emulsion breaking for As, Se and Hg determination in crude palm oil by vapor generation-AFS. *Food Chemistry, 318* (February). https://doi.org/10.1016/j.foodchem.2020.126473

Sulihatimarsyila, A. W. N., Lau, H. L. N., Nabilah, K. M., & Azreena, I. N. (2020). Production of re fined red palm-pressed fibre oil from physical refining pilot plant. *Case Studies in Chemical and Environmental Engineering, 2*(June).

Sun, X., Zhang, L., Yan, J., Song, F., Tian, S., & Xie, J. (2021). Effects of enzymatic free fatty acid reduction process on the composition and phytochemicals of rice bran oil. *Food Chemistry, 337*(February 2020). https://doi.org/10.1016/j.foodchem.2020.127757

Tang, T., Cao, S., Xi, C., Li, X., Zhang, L., Wang, G., & Chen, Z. (2020). Chitosan functionalized magnetic graphene oxide nanocomposite for the sensitive and effective determination of alkaloids in hotpot. *International Journal of Biological Macromolecules, 146*, 343–352. https://doi.org/10.1016/j.ijbiomac.2019.12.259

Teh, S. S., & Lau, H. L. N. (2021). Quality assessment of refined red palm-pressed mesocarp olein. *Food Chemistry, 340*(August 2020). https://doi.org/10.1016/j.foodchem.2020.127912

Tian, Y., Zhou, X., Lin, S., Ji, X., Bai, J., & Xu, M. (2018). Syngas production from air-steam gasification of biomass with natural catalysts. *Science of the Total Environment, 645*, 518–523. https://doi.org/10.1016/j.scitotenv.2018.07.071

Werth, K., Kaupenjohann, P., Knierbein, M., & Skiborowski, M. (2017). Solvent recovery and deacidification by organic solvent nanofiltration: Experimental investigation and mass transfer modeling. *Journal of Membrane Science, 528*(June 2016), 369–380. https://doi.org/10.1016/j.memsci.2017.01.021

Yahaya, M., Ramli, I., Muhamad, E. N., Ishak, N. S., Nda-Umar, U. I., & Taufiq-Yap, Y. H. (2020). K2O doped dolomite as heterogeneous catalyst for fatty acid methyl ester production from palm oil. *Catalysts, 10*(7), 1–17. https://doi.org/10.3390/catal10070791

Zhang, F., Wang, M., & Yang, M. (2021). Successful application of the Taguchi method to simulated soil erosion experiments at the slope scale under various conditions. *Catena, 196*(July 2020), 104835. https://doi.org/10.1016/j.catena.2020.104835

Zhou, J., Ma, Y., Jia, Y., Pang, M., Cheng, G., & Cai, S. (2019). Phenolic profiles, antioxidant activities and cytoprotective effects of different phenolic fractions from oil palm (Elaeis guineensis Jacq.) fruits treated by ultra-high pressure. *Food Chemistry, 288*(March), 68–77. https://doi.org/10.1016/j.foodchem.2019.03.002